Surface photochemistry of CO adsorbed on alumina supported nanoparticulate platinum

2010 J. Phys.: Condens. Matter 22 084011

(http://iopscience.iop.org/0953-8984/22/8/084011)

J. Phys.: Condens. Matter **22** (2010) 159802 (1pp) doi:10.1088/0953-8984/22/15/159802

Corrigendum

Surface photochemistry of CO adsorbed at alumina supported nanoparticulate platinum

A Al-Shemmary, R Buchwald and K Al-Shamery

2010 *J. Phys.: Condens. Matter* **22** 084011

We have noticed an error in our paper. In the caption of figure 1 and in the text (page 3, right column, line 5 of text) the laser fluence indicated should be 19.1 mJ cm^{-2} instead of the written 6.4 mJ cm^{-2}.

J. Phys.: Condens. Matter **22** (2010) 084011 (6pp) doi:10.1088/0953-8984/22/8/084011

Surface photochemistry of CO adsorbed on alumina supported nanoparticulate platinum

A Al-Shemmary, R Buchwald and K Al-Shamery

Carl von Ossietzky Universität Oldenburg, Institute for Pure and Applied Chemistry and Centre of Interface Science, PO Box 2503, D-26111 Oldenburg, Germany

E-mail: katharina.al.shamery@uni-oldenburg.de

Received 1 July 2009, in final form 11 September 2009
Published 4 February 2010
Online at stacks.iop.org/JPhysCM/22/084011

Abstract

Laser induced desorption of CO adsorbed on platinum nanoparticles on an epitaxial alumina support grown on NiAl(110) is reported for nanosecond laser excitation at $\lambda = 355$ nm. The nominal amount of platinum deposited was 0.1 nm, resulting in platinum particles with an average diameter of a few nanometres. The laser fluence was systematically varied between 6.4 and 25.5 mJ cm^{-2} per pulse. Fourier transform infrared reflection absorption spectra have been recorded as a function of CO coverage, the laser fluence and the number of photons impinging on the surface. Laser desorption is observed, in contrast to the case for experiments on Pt(111) for the same laser wavelength. For laser fluences below 12.7 mJ cm^{-2} per pulse, a cross section of $(1.1 \pm 0.2) \times 10^{-19}$ cm^2 can be estimated from the measurements. At elevated fluences a second desorption channel occurs with a cross section more than an order of magnitude larger, scaling linearly with the laser fluence. In all cases desorption ends at a critical coverage beyond which no desorption occurs and which depends on the laser fluence. Laser induced particle morphology changes are observed for higher laser fluences which are not apparent for bare particles. A model implying energy pooling within adsorbates at hot spots and even spillover between the metal nanoparticles and the oxidic support is discussed. Implications for the design of photocatalysts with possible use in chemical solar energy conversion are pointed out.

1. Introduction

One of the key problems of the next century is to develop strategies for meeting the demand for energy in a permanently growing world population. In this context the chemical storage of solar energy is a promising approach as a sustainable energy resource. The usual approach to produce solar fuels involves the use of photochemical reactions at solid surfaces. For several decades by now semiconductor surfaces have been investigated (Kamat 2007). Most recently it has been found that a surface modification with metal nanoparticles may enhance the efficiency of photochemical cross sections in this context (Pan *et al* 2007). However, surprisingly little is known about the elementary processes of the photochemistry at model metal nanoparticle/oxid support systems (see reviews on most recent work in Watanabe *et al* (2006), Al-Shamery (2006)).

In an early work by Watanabe *et al* (1999) it has been shown that the population of different possible photochemical reaction channels depends on the metal particle size. They have reported that the branching ratio between UV-laser induced photodissociation and photodesorption changes dramatically with the metal particle size for nanoparticles in the lower nanometre regime when looking at the photodissociation of methane adsorbed at nanoparticulate palladium on an epitaxial alumina support. While methane tends to dissociate after laser excitation when adsorbed at larger particles photodesorption is most efficient for smaller nanoparticles at particle diameters below 4.5 nm. Photodesorption becomes particularly efficient when the particle size is in the size regime of the mean free path of the excited electron or below.

Kampling *et al* (2002) used quantum state resolved spectroscopy to map the energy partitioning of NO desorbed from palladium nanoparticles on an epitaxial alumina support. They found that though the photodesorption cross sections easily change by at least one order of magnitude the final energy distribution was little sensitive to the particle size.

From these findings they concluded that apparently defect sites may play a major role to pin the initial excitation energy for inducing the photochemical desorption.

Wille and Al-Shamery (2003a) and Wille *et al* (2003b) investigated local site changes of CO adsorbed at palladium nanoparticles on an epitaxial alumina support. When using ultrashort pulses of laser light they found metal nanoparticle deterioration for CO coverages of fluctuating adsorbate densities (Wille *et al* 2004). From extensive experiments with various isotopic $C^{12}O/C^{13}O$ mixtures they concluded that at particle edges energy pooling arises along rows of densely packed adsorbates which may be followed by energy pinning at kinks and concomitant formation of local hot spots responsible for the metal nanoparticle destruction. The adsorbate coverage was crucial for particle decomposition to occur. For the system investigated desorption was only a minor reaction channel for extremely small particles consisting of only a few atoms.

In view of these results we were interested in investigations of a closely related adsorbate system: CO adsorbed at nanoparticulate platinum on an epitaxial alumina support. In contrast to palladium CO adsorbs on Pt(111) preferentially at on top sites while at Pd(111) it initially adsorbs at threefold coordinated sites at low coverages (Hayden and Bradshaw 1983).

Laser induced desorption of CO from Pt(001) and Pt(111) has been investigated by Peremans *et al* (1993a, 1993b) and Fukutani *et al* (1995) involving a state resolved mapping of the desorbing molecules using (2 + 1) REMPI. The fluence dependence of the desorption with a laser wavelength of 193 nm indicated that CO desorption occurs as a three photon process from Pt(001). This may be connected to a direct excitation of CO itself. On the other hand a single photon process is relevant for CO desorption from Pt(111) indicating an initial surface excitation step. Electron stimulated desorption experiments from Pt(111) by Burns *et al* (1987) resulted in neutral, electronically excited CO. No laser experiments have been reported for nanoparticulate platinum under well defined conditions to our knowledge.

2. Experimental details

The experiments were carried out in a UHV chamber ($p < 2 \times 10^{-10}$ mbar) equipped with a mass spectrometer (Pfeiffer, Prisma) for temperature programmed desorption (TPD) and residual gas analysis and a low-energy electron diffraction system (LEED, Specs ErLEED 1000-A). A NiAl(110) single crystal (MaTecK) was used and cooled to 90 K using liquid nitrogen. Repeated cycles of argon-ion bombardment (sputter gun, DenTec: 900 eV, 4–5 μA) and annealing were used to clean the NiAl(110). An Al_2O_3 epitaxial film was prepared before each experiment by oxidizing the NiAl(110) at $T = 550$ K in 10^{-6} mbar of oxygen and subsequent annealing of the oxide to $T = 1130$ K for 5 min according to a well established procedure known from the literature (Jaeger *et al* (1991) and Libuda *et al* (1994)). The alumina film has a thickness of 5 Å.

Platinum was deposited on the Al_2O_3 using an electron beam evaporator EBV20 from Omnivac with a high purity platinum wire wrapped by a tungsten filament. The thickness of the deposited platinum was calibrated using a quartz microbalance and quartz crystal monitor IL 150 (produced by Intellemetrics Ltd). Note that a nominal monolayer of platinum corresponds to a deposition of 0.226 nm for a full monoatomic coverage. However, platinum forms islands on epitaxial alumina. The growth of platinum clusters deposited on epitaxial alumina grown on NiAl(110) has been investigated by Bäumer *et al* (1995) using scanning tunnelling microscopy (STM) and by Klimenkov *et al* (2003) using transmission electron microscopy (TEM). Klimenkov *et al* found that the average cluster size increases monotonically with increasing coverage while the cluster density exhibits a maximum for a coverage at 0.5 of a monolayer (nominal thickness according to quartz microbalance calibration). Three-dimensional growth is observed with the mean cluster height scaling also linearly with the cluster size. For a deposition of 0.5 of a monolayer they found a cluster density of 9.8×10^{12} cm^{-2} with an average cluster height of 0.7 nm and an average cluster size of 1.39 nm for a surface temperature of 300 K during deposition. We have verified the growth by means of *ex situ* atomic force microscopy (AFM). From particle height measurements with AFM we systematically found larger particles than reported by Klimenkov *et al* by at least a factor of two for equal deposition amounts. We attribute the differences between the literature experiments and our findings to the limitations by our experimental set up, i.e. tip restrictions from AFM and limitations of our quartz microbalance for which the read out accuracy of the monitor is 0.1 nm. The low coverage has been estimated by extrapolating the evaporation time for a certain amount of platinum at a constant flux assuming linear deposition behaviour. The flux measured within the evaporator and the resulting deposition rate have been calibrated by means of the quartz microbalance for larger amounts of platinum deposited. In view of our discrepancy to the literature data we prefer to report the overall number of platinum deposited instead of average particle sizes in the following. The growth of the metal particles is reported to be heterogeneous. Therefore we exclude the discrepancy as being due to a slower deposition rate (by a factor of 10–20 times with a deposition rate of about 0.3–0.4 nm h^{-1}) compared to the one reported by Klimenkov *et al* (2003). In homogeneous growth such a change in deposition rate may result in larger particles.

For recording Fourier transform infrared reflection absorption spectra we used an FT-IR spectrometer BRUKER IFS66. CO was dosed via background dosing at a background pressure of 10^{-8} mbar at liquid nitrogen temperature of the crystal (1 L = 1.33×10^{-6} mbar s). The UV-laser experiments were carried out using a pulsed Nd:YAG laser GCR 130 (Spectra) at 355 nm with 5–6 ns pulse duration. The laser intensity was calibrated by means of a Gentec ED-200. The laser passed through a CaF_2 window and irradiated the sample at normal incidence with p-polarization. The laser fluence of each single laser pulse will be given in the text and varied between 6.4 and 25.5 mJ cm^{-2} per pulse.

3. Results

A saturation coverage of CO adsorbed at a Pt(111) crystal was irradiated with laser light at $\lambda = 355$ nm with up to 1.33×10^{20}

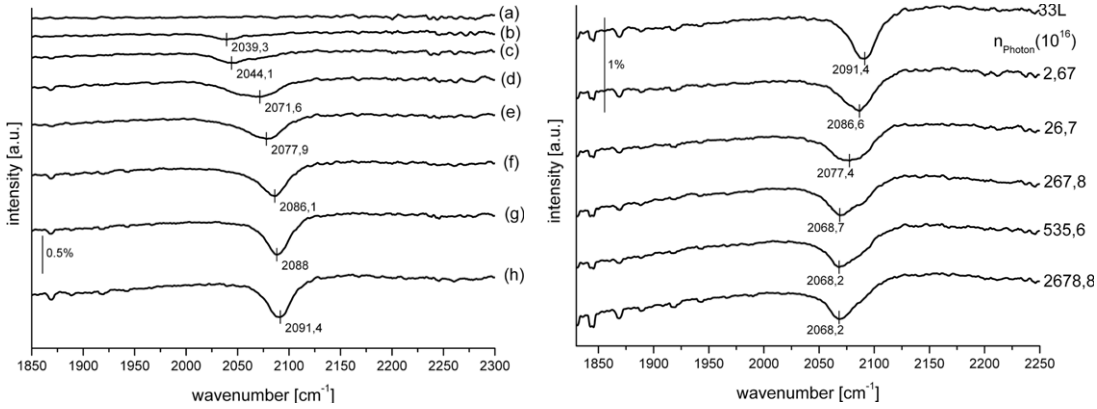

Figure 1. 0.1 nm platinum deposited at $T = 300$ K onto an epitaxial alumina film. *Left:* FT-IRRA spectra in the CO stretching vibration region recorded at $T = 90$ K as a function of CO coverage: (a) 0 L, (b) 0.25 L, (c) 0.5 L, (d) 1 L, (e) 1.25 L, (f) 1.5 L, (g) 2 L, (h) 33 L. *Right:* FT-IRRA spectra of a saturation coverage of CO (33 L) in the CO stretching vibration region as a function of laser irradiation at $\lambda = 355$ nm with overall amount of photons such as indicated and a laser fluence of 6.4 mJ cm^{-2} per laser pulse.

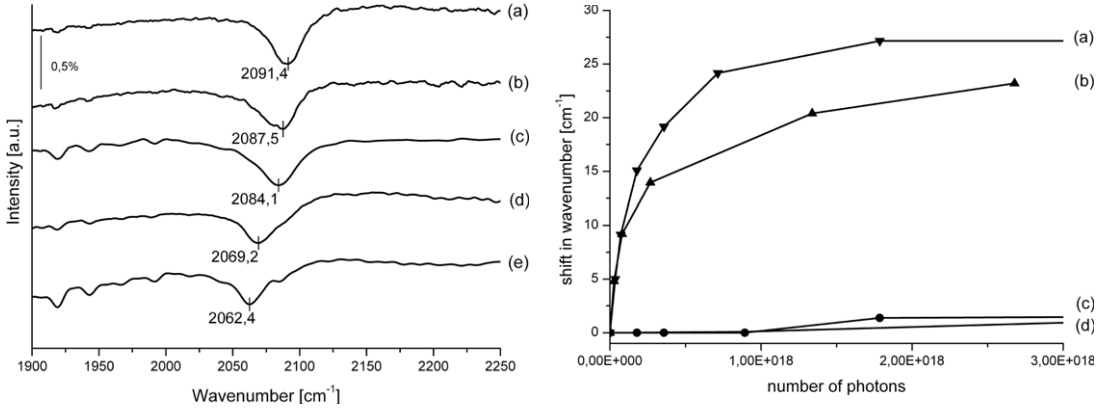

Figure 2. *Left:* FT-IRRA spectra in the CO stretching vibration region adsorbed at 0.1 nm platinum on an epitaxial alumina film after extensive laser irradiation at $\lambda = 355$ nm exhibiting the final state of the experiment. (a) 33 L CO, (b) 6.4 mJ cm^{-2} per pulse (exposure to 1.78×10^{19} photons), (c)12.7 mJ cm^{-2} per pulse (exposure to 1.78×10^{19} photons), (d) 19.1 mJ cm^{-2} per pulse (exposure to 2.67×10^{18} photons), (e) 25.5 mJ cm^{-2} per pulse (exposure to 3.57×10^{18}). *Right:* shift of the peak maximum of the CO stretching vibration relative to the initial saturation coverage and as a function of laser fluence and total amount of photons impinged onto the surface (other conditions as above) (a) 25.5 mJ cm^{-2} per pulse, (b) 19.1 mJ cm^{-2} per pulse, (c) 12.7 mJ cm^{-2} per pulse, (d) 6.4 mJ cm^{-2} per pulse.

photons and laser fluences up to 25 mJ cm^{-2} per pulse. No changes could be observed in our FT-IRRA spectra for the CO signals indicating that laser desorption is not efficient at 355 nm in contrast to the data from Fukutani *et al* (1995) at 193 nm.

Figure 1 (left) exhibits FT-IRRA spectra in the CO stretching vibration region of CO dosed onto nominal 0.1 nm platinum (0.44 ML) on an epitaxial alumina support grown on NiAl(110). The spectra shown have been recorded for increasing coverages between 0.25 and 33 L. For rather low coverages one spectral feature is observed at 2039.4 cm^{-1}. At 1 L a second feature dominates the spectrum peaking at 2071.7 cm^{-1} which is typical for on top CO. With increasing coverage the frequency of the peak maximum shifts to 2091.4 cm^{-1} at 33 L which may be attributed to dipole–dipole coupling. If judging from the peak maximum, one would estimate that saturation of the monolayer coverage is reached at 2 L, however between 2 and 3 L the peak position still exhibits a measurable shift by 3.4 cm^{-1}. To assure a saturation coverage 33 L were dosed.

Figure 1 (right) shows a series of FT-IRRA spectra in the CO stretching vibration region of a saturation coverage of CO exposed to laser irradiation at $\lambda = 355$ nm with an overall amount of photons such as indicated and a laser fluence of 6.4 mJ cm^{-2} per laser pulse. As it is obvious from the spectra the intensity of the FT-IRRA spectra decreases and is accompanied by a shift of the peak maximum from 2091.4 to 2068.2 cm^{-1}. There are no changes apparent for further laser exposure. The spectrum obtained for an exposure to 2.68×10^{19} photons corresponds to a final state of the system for this laser fluence with a coverage resulting in an IR spectrum peaking at 2068.2 cm^{-1}.

This apparent final state depends on the laser fluence used in the experiments as shown in figure 2. The left spectrum exhibits the FT-IRRA spectra of CO adsorbed at 0.1 nm platinum (nominal thickness, deposited at 300 K) on epitaxial alumina. The CO stretching vibration region is shown after exposing a saturation coverage of CO of 33 L dosed at $T = 90$ K to laser pulses of various fluences between 6.4 and 25.5 mJ cm^{-2} per pulse. The overall amount of photons

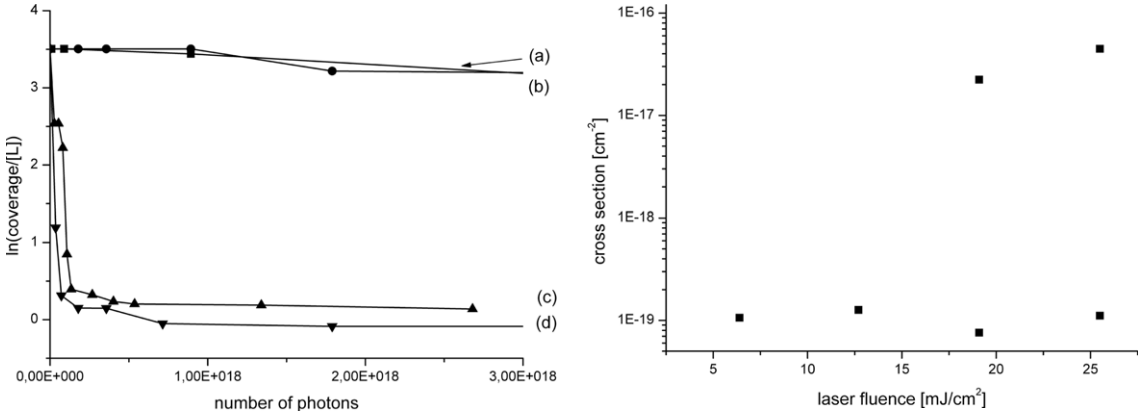

Figure 3. *Left*: logarithmic plot of the coverage of CO (extrapolated from frequency shifts of figure 1) as a function of photons impinged onto the surface (nominal 0.1 nm platinum on an epitaxial alumina film at $T = 300$ K, laser irradiation at $\lambda = 355$ nm, crystal temperature during laser experiment: $T = 90$ K). (a) 6.4 mJ cm^{-2} per pulse, (b) 12.7 mJ cm^{-2} per pulse, (c) 19.1 mJ cm^{-2} per pulse, (d) 25.5 mJ cm^{-2} per pulse. *Right:* desorption cross sections for CO as a function of laser fluence.

impinged onto the surface which is necessary to reach the final state depends on the laser fluence and ranges from 1.78×10^{19} photons to 2.67×10^{18} with increasing laser fluence. The right graph depicts the corresponding shift of the CO stretching vibration peak as a function of the number of photons impinged onto the surface for various laser fluences used. Although one has to be careful with relating IR intensities to a certain coverage, both peak shifts and intensity changes, indicate a substantial desorption of CO with increasing laser fluence. This is in contrast to our experiments on Pt(111).

The data have been analysed in more detail. The photo induced IR spectral shifts have been taken to calculate the coverage. For this purpose a series of IR spectra taken as a function of coverage before laser irradiation has been used to calibrate the coverage change of a saturation coverage with laser exposure. This analysis assumes a sticking probability of one. The frequency shifts are more sensitive to the CO coverage than IR intensities which exhibit saturation of the intensity before reaching the full coverage. Figure 3 (left) exhibits the plots of the logarithm of the coverages (given in Langmuir) as a function of photons impinged onto the surface. Assuming a desorption process with a first order kinetics the desorption cross section of the laser induced desorption may be extracted using the equation

$$\ln(N/N_0) = -\sigma n_{\mathrm{ph}} \qquad (1)$$

with N being the amount of molecules remaining on the surface, N_0 being the initial coverage, σ being the desorption cross section and n_{ph} the number of photons impinged onto the surface. While at the two lower laser fluences desorption cross sections of $(1.1 \pm 0.2) \times 10^{-19}$ cm^2 are obtained, the larger laser fluences have to be fitted with a biexponential. For the first laser pulses at high CO coverages one obtains a cross section of $(2.3 \pm 0.2) \times 10^{-17}$ cm^2 for 19.1 mJ cm^{-2} per pulse and $(4.4 \pm 0.2) \times 10^{-17}$ cm^2 for 25.5 mJ cm^{-2} per pulse while for prolonged laser exposure a value similar to the lower laser fluence regime of $(1.1 \pm 0.2) \times 10^{-19}$ cm^2 can be found. The given evaluation of the cross sections assume a sticking probability of one for CO on the Pt nanoparticles and neglect particle modifications. As both factors, the laser fluence and the minimum CO coverage for laser desorption to occur, play a role a simple model considering one or multiphoton processes is not sufficient to explain the findings.

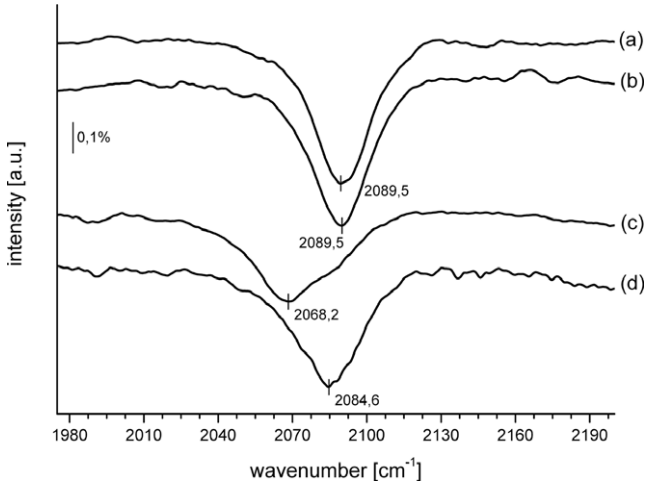

Figure 4. FT-IRRA spectra in the CO stretching vibration region adsorbed onto 0.1 nm platinum at an epitaxial alumina film, laser irradiation at $\lambda = 355$ nm. (a) Initial saturation coverage of 30 L CO without laser irradiation, (b) bare platinum particles irradiated with 2.6×10^{-16} photons (19.1 mJ cm^{-2} per pulse) and covered with 30 L CO after laser irradiation, (c) initial saturation coverage of 30 L CO irradiated with 2.6×10^{-16} photons (19.1 mJ cm^{-2} per pulse) of laser light and (d) initial saturation coverage of 30 L CO irradiated with 2.6×10^{-16} photons (19.1 mJ cm^{-2} per pulse) of laser light and afterwards redosing of 30 L CO.

Furthermore, as shown in figure 4, we observe platinum particle changes at elevated laser fluences which only occur, if the surface is covered with a dense packing of CO. Simple laser irradiation of the bare platinum particles (0.1 nm nominal amount of Pt deposited at 300 K onto alumina) does not modify the particles even at elevated laser fluences (figures 4(a) and (b)). Figure 4(a) exhibits FT-IRRA spectra in the CO stretching vibrational range for an untreated saturation

coverage. Figure 4(b) presents the IR spectra of CO at platinum nanoparticles treated with intense laser light before dosing a saturation coverage of CO. On the other hand figures 4(c) and (d) demonstrate adsorbate induced changes. Figure 4(c) exhibits the final state when irradiating the CO covered nanoparticles intensely with laser light with a fluence of 19.1 mJ cm^{-2} per pulse. In figure 4(d) the CO covered and irradiated particles are recovered with a saturation coverage of CO after the laser irradiation. The found CO spectrum is broadened in comparison to the initial spectrum without laser treatment, the peak intensity has diminished and the CO stretching vibrational frequency has shifted to lower wavelengths. All three findings point towards a particle roughening or even the formation of smaller particles during the laser experiments. This is similar to experiments reported by Wille *et al* (2004) on palladium nanoparticles. As we used the frequency changes as measure for the amount of CO desorbed from the particles we therefore overestimate the desorption efficiency in view of the dependence of the IR signal from the coverage in case of intense laser irradiation.

4. Conclusions

Laser induced desorption of CO is observed from saturation coverages on alumina supported platinum particles in the lower nanometre regime for laser light at $\lambda = 355$ nm with laser fluences between 6.4 and 25.5 mJ cm^{-2} per pulse. Below a critical coverage desorption stops. However, this critical coverage depends on the laser fluence used and is the smaller the larger the laser fluence is. If we only assume a simple model in which a preferential desorption occurs from favoured adsorption sites alone, we shall run into problems to explain the laser fluence dependence. As the local molecular distance is crucial for efficient CO desorption to occur a more plausible explanation involves a strong dipole–dipole coupling of vibrationally excited adsorbate molecules. Here the vibrational excitation is gained through short electronic excitation. A concomitant energy pooling at certain favourable hot spots may then be followed by laser desorption.

Similar to the coherent excitation experiments of Wille *et al* on CO at palladium particles on alumina (Wille *et al* 2004) adsorbate induced roughening if not particle destruction is detected for dense adsorbate coverages at elevated laser fluences.

Within the energy pooling concept pointed out above laser induced roughening is also easy to be understood. Wille *et al* pointed out that hot spots may particularly build up at edges and kinks. Such a prominent role of local effects at lower coordinated metal particle sites has also been reported by Kampling *et al* (2002) for the quantum state resolved mapping of the energy partitioning in desorbing NO molecules from palladium nanoparticles. Fluence depending field enhancement effects at small particles or low coordinated particle sites may also play a further role.

A second interpretation for the observed adsorbate involving particle modifications is that a sort of photobleaching occurs from desorption of photochemically formed platinum carbonyls. However, no typical carbonyl bands in the IR are to be found. This is why we do not follow this possible explanation.

Besides particle changes a sudden increase of the desorption efficiency by more than one order of magnitude for elevated laser fluences is remarkable. The onset of two or three photon processes at elevated fluences would imply a nonlinear though smoother change in desorption yields. This might indicate a spillover from CO molecules adsorbed at the platinum nanoparticles to the alumina support followed by desorption from the only weak interacting oxide surface. If further investigations support such a possible spillover effect this finding is particularly relevant for metal/support systems discussed in chemical solar energy conversion in which the support itself may also play an active role in the ongoing photochemistry.

To summarize, the presented data together with the cited experiments on other systems lead us to the conclusion that apparently two phenomena can be found more generally for a variety of systems. First of all the lowering of the dimensionality of the metal system may foster efficient laser desorption to occur even if the bulk material is not photochemically active when the particle sizes are below the mean free path of the excited electrons within the metal. The second these nanoparticles may photochemically deteriorate in the presence of adsorbates in case the laser fluence exceeds a certain threshold. There are further hints that even spillover processes between the metal nanoparticles and the support may also occur. This latter effect should be followed up in more detail and has been discussed for photochemistry at well defined model systems for the first time in this paper to the best of our knowledge. As real photocatalysis is normally performed under conditions at which high adsorbate densities are to be expected the reported findings have to be carefully considered when designing future photocatalysts.

Acknowledgments

Alaa Al-Shemmary thanks the German Academic Exchange Service (DAAD) for supporting his work with a fellowship. Katharina Al-Shamery is grateful to the German Science Foundation (DFG) who has financed the work within the priority programme SPP 1093 and the State of Lower Saxon for further support. The laser was financed from award money from the Benningson Förder award of the State of North-Rhine Westphalia and is kindly lent by the Ruhr-University of Bochum, Germany.

References

Al-Shamery K 2006 Photochemistry at nanoparticulate surfaces *J. Phys.: Condens. Matter* **18** S1581–601

Bäumer M, Libuda J, Sandell A, Freund H, Graw G, Bertrams T and Neddermeyer H 1995 The grow and properties of Pd and Pt on Al_2O_3/NiAl(110) *Ber. Bunsenges. Phys. Chem. Chem. Phys.* **99** 1381–6

Burns A R, Stechel E B and Jennison D R 1987 Desorption by electronically stimulated adsorbate rotation *Phys. Rev. Lett.* **58** 250–3

Fukutani K, Song M and Murata Y 1995 Photodesorption of CO and CO^+ from Pt(111): mechanism and site specificity *J. Chem. Phys.* **103** 2221–8

Hayden B E and Bradshaw A 1983 The adsorption of CO on Pt(111) studied by infrared reflection absorption spectroscopy *Surf. Sci.* **125** 787–802

Jaeger R, Kuhlenbeck H, Freund H, Wuttig M, Hoffmann W, Franchy R and Ibach H 1991 Formation of a well-ordered aluminium oxide overlayer by oxidation of NiAl(110) *Surf. Sci.* **259** 235–52

Kamat P 2007 Meeting the clean energy demand: nanostructure architectures for solar energy conversion *J. Phys. Chem.* C **111** 2834–60

Kampling M, Al-Shamery K, Freund H, Wilde M, Fukutani K and Murata Y 2002 Surface photochemistry on confined systems: UV-laser-induced photodesorption of NO from Pd-nanostructures on Al_2O_3 *Phys. Chem. Chem. Phys.* **4** 2629–37

Klimenkov M, Kuhlenbeck H and Nepijko S 2003 Growth mode of Pt clusters deposited on gamma-Al_2O_3 (111)/NiAl(110): a TEM study *Surf. Sci.* **539** 31–6

Libuda J, Winkelmann F, Baeumer M, Freund H, Bertrams T, Neddermeyer H and Muller K 1994 Structure and defects of an ordered alumina film on NiAl(110) *Surf. Sci.* **318** 61–73

Pan F, Zhang J, Zhang W, Wang T and Cai C 2007 Enhanced photocatalytic activity of Ag microgrid connected TiO_2 nanocrystalline films *Appl. Phys. Lett.* **90** 122114

Peremans A, Fukutani K, Mase K and Murata Y 1993a CO and CO^+ photodesorption from Pt(001) at 193 nm *Phys. Rev.* B **47** 4135–8

Peremans A, Fukutani K, Mase K and Murata Y 1993b UV photodesorption of CO from Pt(001) at 193 nm investigated by state-selective detection *Surf. Sci.* **283** 189–94

Watanabe K, Matsumoto Y, Kampling M, Al-Shamery K and Freund H 1999 Photochemistry of methane on Pd/Al_2O_3 model catalysts: control of photochemistry on transition metal surfaces *Angew. Chem. Int. Edn* **38** 2192–4

Watanabe K, Menzel D, Nilius N and Freund H 2006 Photochemistry on metal nanoparticles *Chem. Rev.* **106** 4301–20

Wille A and Al-Shamery K 2003a size dependence of laser driven processes of adsorbates at supported nanoparticulate metal systems *Surf. Sci.* **528** 230–41

Wille A, Buchwald R and Al-Shamery K 2004 Adsorbate-induced roughening of nanosized palladium particles after coherent laser excitation *Appl. Phys.* A **78** 205–11

Wille A, Haubitz S and Al-Shamery K 2003b Laser induced adsorption site changes of CO adsorbed at nanoparticulate palladium aggregates on an alumina support driven by local adsorbate density fluctuations *Chem. Phys. Lett.* **367** 609–16